

## MAXIMUM LIKELIHOOD-BASED METHOD FOR ANGULAR DIFFERENTIAL IMAGING

Cornia, A.<sup>1,2</sup>, Mugnier, L.<sup>1</sup>, Sauvage, J.-F.<sup>1</sup>, Fusco, T.<sup>1</sup>, Rousset, G.<sup>2</sup> and Védrenne, N.<sup>1</sup>

**Abstract.** In the context of the SPHERE planet finder project, we further develop a recently proposed method, based on detection theory, for the efficient detection of planets using angular differential imaging. The proposed method uses the fact that with the SPHERE instrument the field rotates during the night. The method starts with the appropriate combination of images recorded at different times into so-called pseudo-data. It then uses jointly all these pseudo-data in a Maximum-Likelihood (ML) framework to detect the position and amplitude of potential companions of the observed star, taking into account the mixture of photon and detector noises. The method is validated on simulated data.

### 1 Introduction

The European project SPHERE (Beuzit *et al.* 2008) is the planet searcher of VLT (ESO), based on direct imaging in the near-IR. The goal of SPHERE is to detect warm Jupiters, orbiting sun-like stars at 10 pc from the Sun. To do so, one needs to use an extreme adaptive optics system (XAO) to compensate the atmospheric turbulence which spreads the light of the star, and a high-performance coronagraph to remove the star's photons in order to reduce the noise. But these two techniques alone are not sufficient, because the contrast between the star and the planet at 1.6  $\mu\text{m}$  is close to  $10^6$ . In order to reach the ultimate detection performance needed to detect a warm Jupiter, it is mandatory to combine the abovementioned optical devices to an *a posteriori* processing of all data.

The main problematic is to disentangle the potential companion's signal from the quasi static speckles, which are due to residual aberrations and constitute a major "noise" source. These speckles present the same characteristic angular size as the diffraction element,  $\lambda/D$ , and the same size as the companion's signal. With no more information, it is impossible to discriminate between the speckles and the companion. In order to do so, the SPHERE instrument includes the ability to perform spectral and angular differential imaging.

Spectral differential imaging consists in acquiring simultaneous images of the system star-companion at different wavelengths. The spectral signatures of the exoplanet's atmosphere ensures that the planet's response will significantly vary in the images, while the star response and therefore the speckles remain the same.

Angular differential imaging relies on the fact that, if the pupil is stabilized, the field rotates naturally as the speckle in principle should remain fixed.

If both temporal and spectral channels are available, as is the case with the SPHERE instrument, then one may first combine each pair of simultaneous spectral images into one image so as to enhance the planet's signal, and then use the resulting image series as temporal channels for angular imaging. In this paper, we investigate the joint processing of such temporal series of images.

At least two approaches are possible for this problem:

- jointly estimate the coronagraphic response of the star, and the companion's position and amplitude (or flux). This approach has been adopted by Smith *et al.* (2007);
- numerically remove the star signal, and only estimate the planet (Mugnier *et al.* 2007).

---

<sup>1</sup> ONERA/DOTA, B.P. 72, 92322 Châtillon cedex, France

<sup>2</sup> LESIA, Observatoire de Paris, 5 place Jules Janssen, 92195 Meudon, France

In the framework of the SPHERE project, the static aberrations are likely to evolve during observing time, and the estimation of the star signal should therefore be done several times during night. We therefore choose the second option, which consists in cancelling the star image numerically.

This suppression is done by a pairwise subtraction of sufficiently separated images. Let  $\mathbf{i}_t$  the raw images, the new data are the images differences  $\Delta(\mathbf{r}, k) = \mathbf{i}_{k_1(k)}(\mathbf{r}) - \mathbf{i}_{k_2(k)}(\mathbf{r})$ , where  $k_1(k)$  and  $k_2(k)$  are indices chosen so as to preserve the planet's signal in the difference. The estimation of the companion's position and amplitude is done on these new data, through a Maximum Likelihood approach.

## 2 Maximum-Likelihood estimation for position and amplitude of the companion

In the new data consisting of the  $k_{\max}$  differential images denoted by  $\Delta(\mathbf{r}, k)$ , and assuming that a planet is indeed present, the data model at each pixel  $\mathbf{r}$  of image  $k$  is the following:

$$\Delta(\mathbf{r}, k) = a \cdot \mathbf{p}(\mathbf{r}, k; \mathbf{r}_0) + \mathbf{n}(\mathbf{r}, k), \quad (2.1)$$

where  $a$  is the planet's amplitude and  $\mathbf{r}_0$  is the initial planet's position,  $\mathbf{p}(\mathbf{r}, k; \mathbf{r}_0)$  is the known pattern of the planet in this data for an assumed  $\mathbf{r}_0$  (which is the difference of two PSF's), and  $\mathbf{n}(\mathbf{r}, k)$  denotes the noise.

The maximum likelihood approach consists in searching for  $(\hat{\mathbf{r}}_0, \hat{a})$  that maximize the likelihood  $L(\mathbf{r}_0, a)$ . In the following we assume that the noise is non-homogeneous, Gaussian and white, with variance  $\sigma^2(\mathbf{r}, k)$ . This assumption is reasonable and allows us to take into account both the photon and the detector noises, as done in AO-corrected image restoration (Mugnier *et al.* 2004).

We can define a criterion  $J$  to be maximized, which is linked to the likelihood  $L$  this way:

$$J \triangleq -a^2 \sum_{k, \mathbf{r}} \frac{p^2(\mathbf{r}, k; \mathbf{r}_0)}{\sigma^2(\mathbf{r}, k)} + 2a \sum_{k, \mathbf{r}} \frac{p(\mathbf{r}, k; \mathbf{r}_0) \Delta(\mathbf{r}, k)}{\sigma^2(\mathbf{r}, k)} = - \sum_{k, \mathbf{r}} \frac{|\Delta(\mathbf{r}, k) - a p(\mathbf{r}, k; \mathbf{r}_0)|^2}{2\sigma^2(\mathbf{r}, k)} + \text{const} = 2 \ln L(\mathbf{r}_0, a) + \text{const} \quad (2.2)$$

The optimal value  $\hat{a}(\mathbf{r}_0)$  of  $a$  for each given  $\mathbf{r}_0$  is computable analytically; we can also take into account the fact that the flux always has to be positive:

$$\hat{a}(\mathbf{r}_0) = \max \left( \frac{\sum_{k, \mathbf{r}} p(\mathbf{r}, k; \mathbf{r}_0) \Delta(\mathbf{r}, k) / \sigma^2(\mathbf{r}, k)}{\sum_{k, \mathbf{r}} p^2(\mathbf{r}, k; \mathbf{r}_0) / \sigma^2(\mathbf{r}, k)}, 0 \right). \quad (2.3)$$

The numerator of this expression can be seen as a scalar product (correlation) between the planet's patterns and the images, with weights given by the noise variance. And the denominator is simply a normalization constant.

If we insert this optimal value for the amplitude into metric  $J$ , we obtain an expression of the latter that depends, explicitly at least, only on the sought planet position:

$$J'(\mathbf{r}_0) \triangleq J(\mathbf{r}_0, \hat{a}(\mathbf{r}_0)) = \begin{cases} \frac{(\sum_{k, \mathbf{r}} p(\mathbf{r}, k; \mathbf{r}_0) \Delta(\mathbf{r}, k) / \sigma^2(\mathbf{r}, k))^2}{\sum_{k, \mathbf{r}} p^2(\mathbf{r}, k; \mathbf{r}_0) / \sigma^2(\mathbf{r}, k)} & \text{if } \hat{a}(\mathbf{r}_0) > 0 \\ 0 & \text{if } \hat{a}(\mathbf{r}_0) \leq 0. \end{cases} \quad (2.4)$$

This criterion  $J'$  can be computed for each possible initial planet position on a grid, which can be chosen as the original pixel grid of the images, or as a finer grid if it is useful. The most likely initial planet's position is then  $\hat{\mathbf{r}}_0 = \arg \max J'(\mathbf{r}_0)$ , and the most likely amplitude is  $\hat{a}(\hat{\mathbf{r}}_0)$  as computed with Eq. (2.3).

## 3 Detection criterion

Once the likelihood and amplitude maps are computed, the main problem is to decide which peaks are true companions and which ones are not. One way to do so is to additionally compute the standard deviation of the estimated amplitude,  $\sigma(\hat{a}(\mathbf{r}_0))$ , for each possible planet position  $\mathbf{r}_0$ , *i.e.* to compute how the noise propagates from the images to our amplitude estimator. A possible detection criterion, which can be linked to the probability of false alarm, is then to decide that all positions where the signal-to-noise ratio (SNR) of the estimated amplitude, defined as:

$$\text{SNR}(a) = \hat{a}(\mathbf{r}_0) / \sigma(\hat{a}(\mathbf{r}_0)), \quad (3.1)$$

is greater than some threshold are true detections.

The variance of the estimated flux for a given position  $\mathbf{r}_0$  is computed by means of Eq. (2.3) using the fact that the noise in our images  $\Delta(k, \mathbf{r})$  is white, both temporally and spatially; after some maths we obtain:

$$\sigma^2(\hat{a}(\mathbf{r}_0)) = \left( \sum_{\mathbf{r}, k} \frac{p^2(\mathbf{r}, k; \mathbf{r}_0)}{\sigma^2(\mathbf{r}, k)} \right)^{-1}. \quad (3.2)$$

## 4 Validation by simulation

### 4.1 Simulation conditions

The conditions of simulation are representative of the SPHERE/IRDIS instrument on the VLT: an 8 m telescope, a seeing of  $0.8''$ , a wind speed of 12.5 m/s; a SAXO-like AO system:  $41 \times 41$  actuators, a  $40 \times 40$  sub-aperture Hartmann-Shack wavefront sensor, a sampling frequency of 1200 Hz; residual static aberrations with a standard deviation of  $\sigma_{\phi_u} = 35$  nm upstream of the coronagraph and  $\sigma_{\phi_d} = 100$  nm downstream of the coronagraph. We have assumed a pupil-stabilized mode, with residual aberrations kept constant during the simulated run.

A hundred  $256 \times 256$  images are simulated at an imaging wavelength of  $\lambda = 1.593 \mu\text{m}$  with Poisson (photon) noise. The image of the star is computed by means of the analytical expression for the long-exposure AO-corrected coronagraphic image of a star (Sauvage 2007).

We have simulated seven planets which lie aligned at distances multiple of  $4\lambda/D$  from the central star. The long-exposure AO-corrected images of the planets are computed using the static aberrations and the residual phase structure function, assuming that the planets do not “see” the coronagraph.

The star flux is  $2.67 \cdot 10^7$  ph/s, the planet flux is 28.5 ph/s, which yields a ratio of  $9.36 \cdot 10^5$ . Depending on the simulation, the total exposure time is either 1h or 2h.

### 4.2 Impact of the proposed positivity constraint and of the noise variance map

Fig. 1 shows the improvements brought by the positivity constraint and a non-homogeneous noise variance map: a part of the peaks due to false detections are eliminated by the former, and the remaining are dimmed by the latter.

In order to better quantify the improvement brought by positivity and by the use of an inhomogeneous noise variance map, Fig. 2 shows the SNR of the estimated amplitude (defined by Equation (3.1)) thresholded to value of 4, in the difficult case of a one hour total observation time. In the two cases where a homogeneous noise is assumed in the processing, the noise variance has been taken equal to the spatial average of the empirical variance of each pixel in time.

For the case where both the positivity and the inhomogeneous noise variance map are used, all the true planets are detected and no false alarm is present with the displayed threshold. The corresponding detection map is the boxed one of Fig. 2. For the three other cases, whatever the chosen threshold, in this simulation there are either false alarms (for low threshold values) or undetected planets (for high threshold values).

### 4.3 Impact of the exposure time

As expected, for two hours of total exposure time instead of one, there are less false detections for low thresholds and all planets are detected even for higher threshold values. A more detailed discussion with figures can be found in Mugnier *et al.* (2008).

## 5 Perspectives

Further simulations are to be run to exploit the two spectral channels too, and to test the robustness of the method for slowly varying aberrations.

## References

Beuzit, J.-L., Feldt, M., Dohlen, K., Mouillet, D., Puget, P., & Wildi, F. 2008, in *Adaptive Optics Systems*, 7015, Proc. Soc. Photo-Opt. Instrum. Eng.

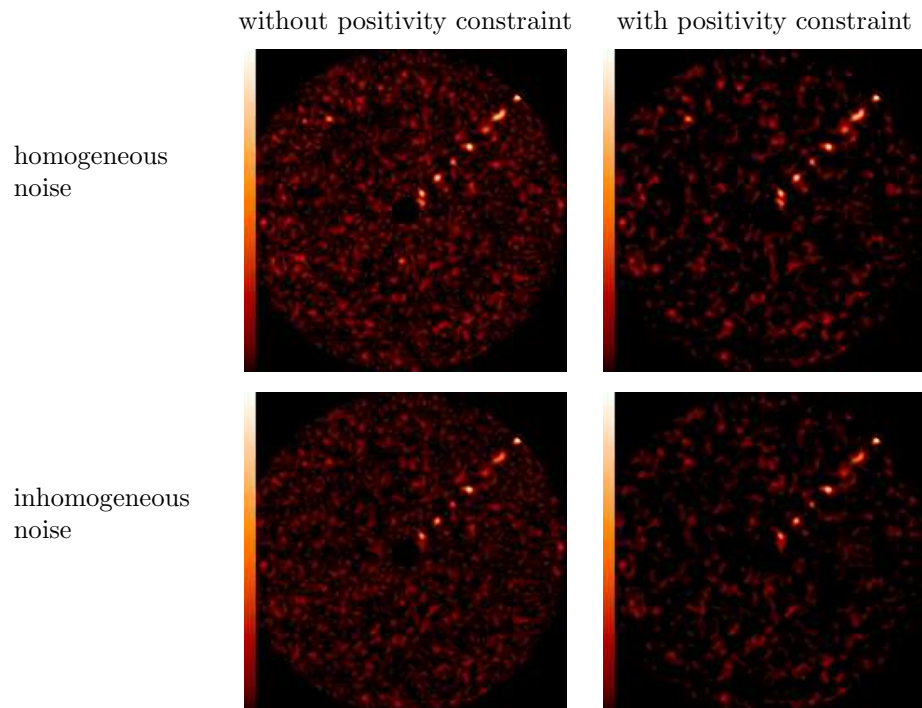


**Fig. 1.** Likelihood maps with 100 images and an exposure time of 1 h. Top row: homogeneous noise. Bottom row: inhomogeneous noise. Left column: without positivity constraint. Right column: with positivity constraint.

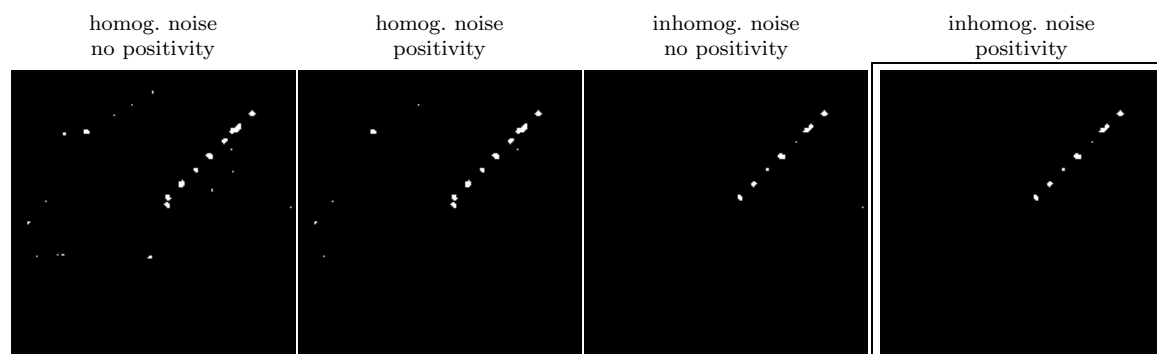


**Fig. 2.** Detection maps obtained by thresholding the maps of the SNR of the estimated flux of Fig. 1 at the value of 4.

Mugnier, L., Sauvage, J.-F., Fusco, T., & Rousset, G. 2007, in *Adaptive Optics: Analysis and Methods*, OSA, June 18–20, 2007, Vancouver (Canada)

Mugnier, L., Fusco, T., & Conan, J.-M. 2004, *J. Opt. Soc. Am. A*, 21, 1841–1854

Sauvage, J.-F. 2007, PhD thesis, Université Paris VII, December 2007

Mugnier, L., Cornia, A., Sauvage, J.-F., Védrenne, N., Fusco, T., & Rousset., G. 2008, in *Astronomical telescopes 2008 SPIE Symposium*, Adaptive Optics Systems Conference, N. Hubin, C. E. Max, and P. L. Wizinowich editors, 7015, June 2008, Marseille (France)